Journal of Materials and Environmental Sciences
ISSN : 2028-2508
CODEN : JMESCN

J. Mater. Environ. Sci., 2018, Volume 9, Issue 4, Page 1324-1334

https://doi.org/10.26872/jmes.2018.9.4.144

http://www.jmaterenvironsci.com

Adsorption of Methylene Blue from Aqueous Solution by Humic Acid Extracted from Freshwater River Humus

E. Inam[1,2*], O. O. Udo[1], J. B. Edet[2,3], U. J. Etim[3], N. O. Offiong[1,2]

[1]*Department of Chemistry, University of Uyo, Uyo, Nigeria.*
[2]*Centre for Energy and Environmental Sustainability Research (CEESR), University of Uyo, Uyo, Nigeria.*
[3]*State Key Laboratory of Heavy Oil Processing, China University of Petroleum, Huadong, 266280, Qingdao, P.R. China*

Received 22Jun 2016,
Revised 21 Oct 2016,
Accepted 25 Oct 2016

Keywords
- ✓ Dye adsorption,
- ✓ Methylene blue,
- ✓ Humic acid,
- ✓ Low-cost adsorbent,
- ✓ Batch technique.

eduinam@uniuyo.edu.ng;
Phone: +2348181750861

Abstract

The extraction and utilization of humic acid (HA) as a low cost adsorbent for the removal of methylene blue (MB) from aqueous solution was investigated. The HA extracted from the sediment of the lower course of a river gave a yield of 4.89%. Characterization of the HA was performed using N_2 adsorption, Fourier transform infra-red spectroscopy (FTIR), X-ray diffraction (XRD) and Ultra-violet visible spectroscopy (UV-vis). Adsorption potential of the prepared HA for the removal of MB from aqueous solution was evaluated by batch method. The results revealed significant adsorption with just 100 mg of HA, suggesting a high adsorption potential. The solution pH was found to influence the adsorption behaviour of the HA, due to the overall negatively charged surface of the adsorbent at high pH. The data obtained from the equilibrium adsorption studies were fitted to Langmuir, Freundlich and Temkin's isotherm models. The adsorption was best described according to the Freundlich's isotherm model (R^2 = 0.971), suggesting a layer by layer adsorption. This study indicates that humic acid could form an eco-friendly low cost adsorbent for the removal of cationic dyes from aqueous solution.

1. Introduction

Water pollution is one of the major factors affecting the quality and quantity of drinking water available for human consumption. This is in addition to the prevailing water scarcity issues currently plaguing some regions of the world, particularly in Africa [1, 2]. These issues have placed water treatment as inevitable means for water reuse and reclamation. The major pollutants that adversely affect the biodiversity, ecosystem functioning as well as human use of water resources include various hazardous organic and inorganic substances [3]. Synthetic dyes are among these groups of pollutants. As a result of their wide application in cosmetic, paper, carpet, food, textile, and printing industries, synthetic dyes have become prominent organic pollutants of aquatic environments, where resulting industrial effluents are discharged. It has been reported that about 30% of applied dyes end up in the effluent [4]. Once in water systems, colouration from dyes hinders light penetration, which influences photosynthetic processes in aquatic planktons [5]. Also, dyes and some of their transformation products may pose several detrimental impacts ranging from aesthetic, mutagenic and carcinogenic effects as well as severe damage to reproductive systems, liver, and dysfunction of the kidney [5, 6]. In addition, increased biological and chemical oxygen demand (BOD and COD) in dye-laden effluents discharged into aquatic ecosystems may reduce the amount of oxygen available for aquatic organisms, which may result in asphyxiation [7].

Methylene blue (MB) in particular is a cationic dye employed basically in the textile industry for a variety of purposes. Chemically, it is a heterocyclic aromatic compound with a molecular formula of $C_{16}H_{18}N_3SCl$ and its structure is given in Figure 1. It is a solid, odourless dark green powder that yields a blue solution when dissolved in water. It is widely used in dyeing fabrics, and as a redox indicator in analytical chemistry. However, it is capable of causing eye burns which may lead to permanent injury to human eyes as well as aquatic animals and also irritates the skin and gastrointestinal tract with symptoms of nausea, vomiting

and diarrhoea [8]. The continuous quest for the treatment of dye-contaminated waters is informed by the fact that their synthetic origin and predominant aromatic moieties are not easily biodegradable [9]. In view of these, several investigations have been carried out to remove methylene blue and indeed other dyes from water. Some physicochemical and biological treatment techniques include coagulation, precipitation, filtration, oxidation, liquid membrane separation, activated sludge processes, and adsorption [10, 11]. Of all the methods studied, adsorption has been viewed as cost effective and efficient [12]. Many authors have reported removal of methylene blue using various adsorbents [13-23].

Most recently, humic acid (HA) and their fabricated composites have been employed to remove some pollutants from aqueous solutions including dyes [24-30]. Humic substances are a major natural organic matter in the soil as well as in geological organic deposits such as lake, sediments, peats, brown coals and shales [31]. As a principal component of humus produced as a result of the biodegradation of dead organic matter, HA shows a high reaction activity due to its unique amorphous structure which possesses large polycyclic aromatic hydrocarbons as framework and a lot of functional groups - carboxyl, phenolic hydroxyl, carbonyl, methoxyl, hydroxyl, etheryl and amino groups on the framework [26].

In spite of the recent attention on HA-based adsorbents, studies focusing on the adsorption of methylene blue by pure HA derived from river sediment are not reported. In addition, the origin and type of bio-remains may alter the properties of HA which influence the behaviour of the final product. Therefore, this research was aimed at extracting HA from the sediment of freshwater ecosystem and ascertaining its efficiency as a low cost adsorbent for the removal of a cationic dye (MB) from aqueous solution by batch process.

2. Material and Methods

2.1. Preparation and characterization of adsorbent

2.1.1.Materials

The reagents used include: MB, sodium hydroxide, hydrochloric acid and silver nitrate. All Chemicals were analytical grade (Sigma Aldrich, UK).

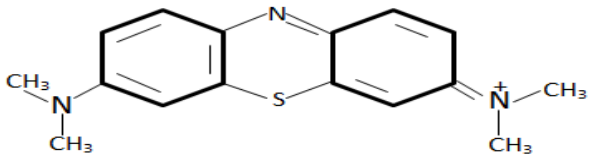

Figure 1: Structure of methylene blue

2.1.2.Preparation of adsorbent

2.1.2.1.Collection of sample and extraction of humic acid

Sediment sample was collected from the lower course of a fresh water river. The sample was analysed for total organic matter employing a method previously reported [32]. HA was extracted according to the method in the literature [33] with modification. About 50 g of the sediment was weighed into a conical flask and treated with 50 mL of 0.1 M HCl to remove calcium and other polyvalent cations, carbonates and to increase the efficiency of extraction. The slurry obtained was extracted with 200 mL of 0.5 M NaOH. The mixture was shaken on an orbital shaker at 120 rpm for 24 h and then allowed to stand overnight. The solution was filtered and the filtrate was reduced to pH 1.0 using 6 M HCl at room temperature with constant stirring. The suspension was left standing overnight to allow the precipitated HA to settle. A brownish-black coloured solid settled to the bottom of the flask was separated from the supernatant, washed with double distilled water until a negative chloride test with silver nitrate was obtained. The HA obtained was re-surried in NaOH, then centrifuged at 4000 rpm for 15 min for further purification. The final solid product was dried in an oven at 110 ^{o}C for 6 h. The yield of the HA obtained was calculated using the formula:

$$HA\ yield = \frac{w}{w_o} x100 \qquad (1)$$

Where, w is the weight of the dried HA and w_o is the weight of the sediment. The entire experiment was repeated using different extractant concentrations.

2.1.2.2.Purification of commercial humic acid

Commercial humic acid (CHA) was supplied by Aldrich chemicals Co., UK, in the form of the technical grade sodium humate. Before use, the sodium humate was purified to remove sodium and other polyvalent ions present as impurities using the method described by Warwick *et al.* [34]. Exactly 2 g of the Na-form CHA was

dissolved in 1 mL deionized water containing approximately 10 mL of 0.1 M NaOH. The solution was shaken for about 12 h to ensure complete dissolution. The pH of the solution was then lowered to about 1.0 by addition of 6 M concentrated HCl. The solution was left overnight to precipitate, the supernatant solution was decanted off and the HA was re-dissolved in NaOH solution. The whole process of dissolution in NaOH, precipitation with HCl and overnight standing was repeated twice. After the second time, the solution was centrifuged at 4000 rpm for 15 min and the precipitated HA was washed several times with double distilled water until a negative chloride test with silver nitrate was confirmed. The HA was then dried in oven at110 °C for 6 h.

2.2.Characterization

Absorption characteristic of the prepared HA was measured using a UV-vis spectrophotometer (Jenway 73 Series). The data obtained were used for the determination of the degree of humification (Δlog K) and degree of condensation of aromatic structures represented as E4/E6, where E4 and E6 refer to the wavelengths of absorption at 465 and 665 nm, respectively, according to Purmalis and Klavins [35]. The determination of the surface functional groups was carried out using FTIR spectrophotometer (Fisher Thermoscientific, USA) following standard procedures. The spectra were recorded using KBr wafers in the range 4000 cm^{-1} to 400 cm^{-1}. The surface area and porosity analyses were carried out using micrometrics surface area and porosity analyser (Micromeritics Tristar 3000) by nitrogen adsorption method at -77 K. The surface area and pore volume were calculated by BET and t-plot methods, respectively. The pore size analysis was carried out to determine the distribution of pores of the adsorbent. X-ray diffraction pattern was obtained on an X'Pert PRO MPD diffractometer at 40 mA and 40 kV using Cu Kα radiation with a speed of 10°/min from 5° to 75°.

2.3.Adsorption Experiments

About 1 g of MB dye was accurately weighed and dissolved in distilled water in a 1000 mL volumetric flask and made up to the mark. Working solutions were obtained by dilution of the stock solution. In order to investigate the effect of increasing adsorbent concentration on the removal of MB from solution, different HA dosages ranging from 20mg to 800mg were separately shaken in 30 mL of 30 mg/L dye solutions on a platform shaker at 180 rpm. The sample solutions were centrifuged and the supernatants were collected and analysed using UV spectrophotometer at 661 nm. To study the effect of MB concentration, exactly 50mg of the extracted HA was added to 30 mL of different dye concentrations ranging from 2 to 30 mg/L in Erlenmeyer flasks and shaken at 180 rpm. The effect of pH on MB adsorption onto HA was investigated over the range of 2.0 to 12.0. NaOH and HCl, 1.0 M each were used to adjust the dye solutions to the desired pH. A mass of the adsorbent (100mg) was added to 30 mL of a fixed dye concentration at room temperature (29 ± 1 °C) and shaken on a platform shaker at a constant speed of 180 rpm for 30 min. The sample solution was allowed to settle and the supernatant was collected after centrifugation and analysed for residual dye content.

3. Results and Discussion

3.1. Yield of extracted humic acid

Table 1: Yield of humic acid from river sediment

Sediment	Extractant concentration	Yield (%)
	0.1 M	0.20
	0.5 M	4.89
Organic matter content (%)	-	10.1

The yields of the extracted humic acid (EHA) from the river sediment for two different concentrations of extractant are presented in Table 1. The yield increased significantly with an increase in the concentration of extractant. The amount increased about 24 folds when NaOH concentration was increased from 0.1 to 0.5 M. However, concentration of NaOH higher than 0.5 M led to significant chemical changes in the extract. The low yield of the EHA could be due to the low organic matter content in the river sediment, and the enhanced intermolecular forces binding fulvic acids to HAs, such as hydrogen bonding or ester-type linkages [31].

3.2. Characterization of the extracted humic acid

3.1.1. Textural characterization

The specific surface area (calculated by BET method) and the porous nature of the EHA were measured to determine the adsorption property of the adsorbent. The results are summarized in Table 2.

Table 2: Textural properties of EHA

Parameters	Value
BET surface area	156 m^2/g
Micropore area	128 m^2/g
Mesopore area	28 m^2/g
Total pore volume	0.11 cm^3/g
Micropore volume	0.07 cm^3/g
Mesopore volume	0.04 cm^3/g

The quantitative results revealed about 82% of the surface area belong to micropores of the adsorbent, with a micropore volume of 0.07 cm^3/g. This high micropore area, however, is not reflective of the nature of the isotherm for microporous materials [36]. In the guide, the isotherm should be concave to the x-axis. However, the nitrogen adsorption isotherm of EHA (Figure 2) presents a different nature from the IUPAC classifications, suggesting uniqueness of the gas adsorption property of this material. The isotherm showed a large range of hysteresis from 0 - 0.98 P/Po, with no apparent point of coincidence for adsorption and desorption branches, suggesting that the sample had a wide distribution of pore size, from micropores to macropores. This rather strange pore property may be due to HA being a complex material, similar to metal organic framework (MOF) [37]. Nevertheless, the hysteresis loop at the low relative pressure closely resembles that of extracted HAin a previous report [38].

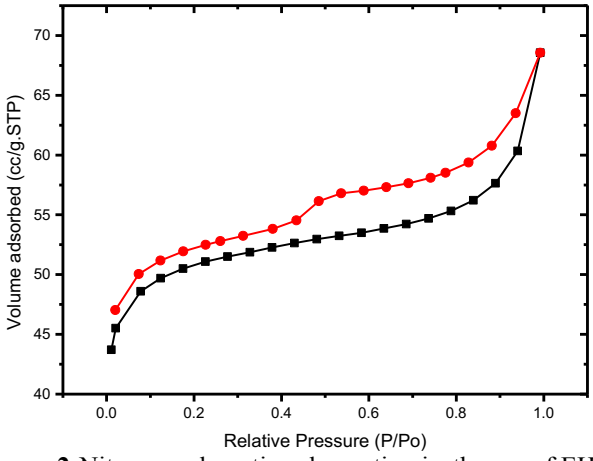

Figure 2: Nitrogen adsorption-desorption isotherms of EHA

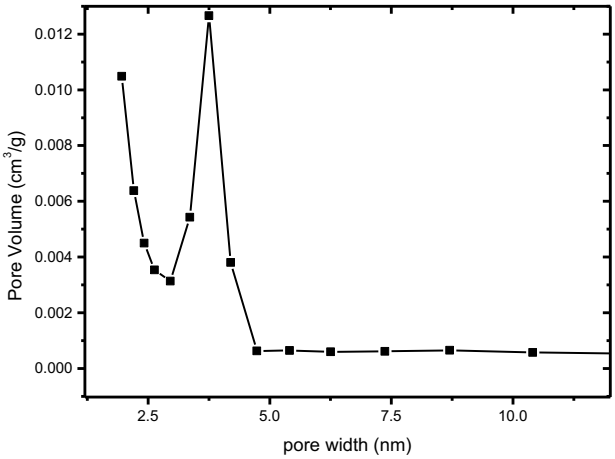

Figure 1: Pore size distribution plot of EHA

Figure 3 shows the BJH pore size distribution of the EHA. The figure indicates a narrow mesopore size distribution with maximum at 3.75 nm. It is of note that our BET instrument is incapable of measuring the micropore size distribution and hence, only pore size in the mesopore region is exhibited.

3.2.2.Spectroscopic analyses and X-ray diffraction

The EHA was analysed by UV-vis and FTIR spectroscopies to determine its characteristic properties and to compare with those of CHA. The UV-vis spectra of the EHA and CHA (figures not shown) were used to determine the degree of humification (Δlog K) and degree of condensation (E_4/E_6) of aromatic structures. The degree of humification was determined by measuring the absorbances at 400 and 600 nm and subsequently expressed in terms of the difference between the log of these two absorbances [35, 39], while the ratio of E_4 and E_6 were obtained by taking the absorbanceat 465 and 665 nm, respectively:

$$\Delta \log K = \log A_{400} - \log A_{600} \quad (2)$$

Table 2: Degree of humification and condensation for EHA and CHA

Sample	Δ Log K	E_4/E_6
EHA	0.81	10.7
CHA	1.09	22.7

The absorbance at 465 nm is indicative of the presence of HAs formed in initial humification stage and that at 665 nm signifies presence of HAs formed in well-humified organic matter [39]. Table 3 shows that the ratio of

the absorbances at 465 and 665 nm (E_4/E_6) of the EHA is lower than that of CHA. Compared with CHA, EHA had higher molecular weights and higher degree of condensation of aromatic constituents [40]. Humic acids could be grouped into three basic classes based on the degree of humification namely; type A, type B and type C, having their Δlog K values as 0.6, 0.6-0.8 and 0.8-1.1, respectively [39, 35]. The Δlog K values of both the EHA and CHA are within the range of 0.8-1.1, indicating that they are type C humic acids. Typically, this value is higher for non-humified material indicating the presence of proteins and carbohydrates in the structure of HA which increases the absorption in the UV region of the spectrum.

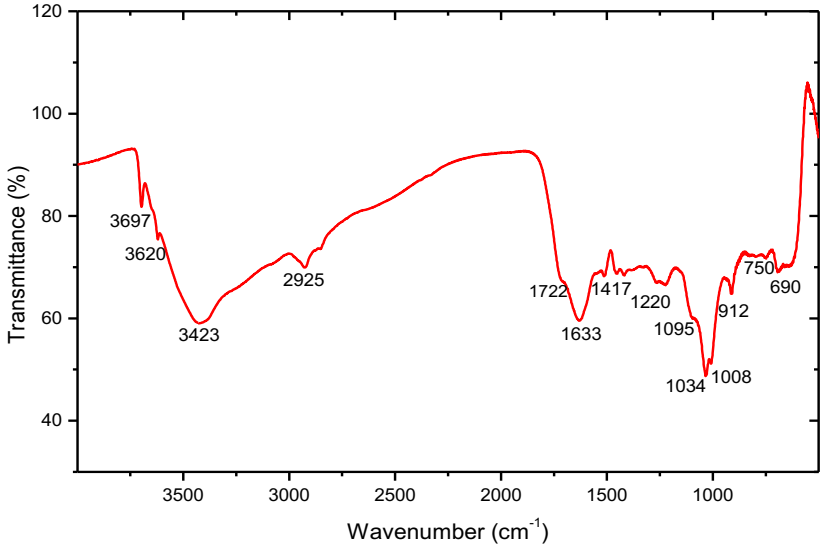

Figure2: IR spectrum of extracted humic acid

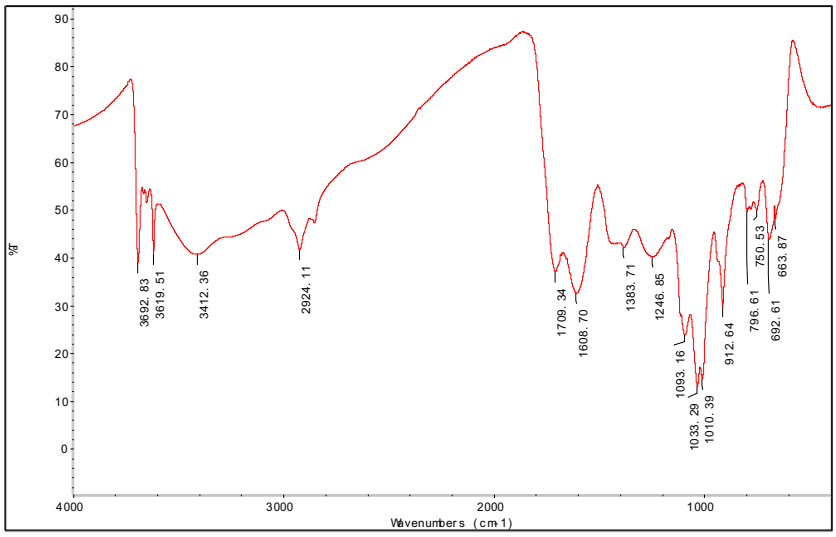

Figure 3: IR spectrum of commercial humic acid

The FTIR spectra of EHA and CHA, in the region between 500 cm^{-1} and 4000 cm^{-1} are shown in Figures 4 and 5, respectively. Comparing the spectra, the EHA presents features which match those of the CHA, indicating the high purity of our prepared sample. Both spectra show series of and corresponding peaks, which indicate similar functional groups are present. The peaks exhibited by both EHA and CHA and their wavenumbers are summarized in Table 4. The spectra are characterized by many peaks, which show the presence of several functional groups due to the complex structure of HAs [41, 42]. From the spectra, the existence of aluminosilicate surface groups (Si-O and Al-OH) implies that there exist residual layers of clay in the HAs [41]. Also, the observable slight shifts in the positions and the reduced intensities of the absorption peaks in EHA compared to CHA could be due to different synthesis conditions and/or different FTIR spectroscopy analysis. The XRD (Figure 6) gives a characteristic of amorphous materials dominated by the residual layers of clay (silicate and apatite) in conformation to the FTIR results.

Table 3: FTIR adsorption bands and functional groups of CHA and EHA

Band position (cm^{-1})		Functional groups
CHA	**EHA**	
690	690	Si-O
750	750	C-H from o-aromatic ring
796	-	Si-O in quartz
912	912	Al-OH
1010	1008	C-O of aromatic ether
1033	1034	Si-O
1093	1095	Si-O stretch bonding
1246	1220	C-O stretch bonding in carboxylic acids, alkyl ether
1384	-	COO^- symmetric stretch, C-O stretch deformation
-	1417	CH_3 asymmetric bending
1608	1633	C-C ring stretch in aromatic
1709	1722	C=O in carboxylic acids and esters
2924	2925	CH_3, CH_2 asymmetric / symmetric stretch
3412	3423	OH in phenols, alcohols and acids
3619	3620	Al-OH stretch
3692	3697	Al-OH stretch

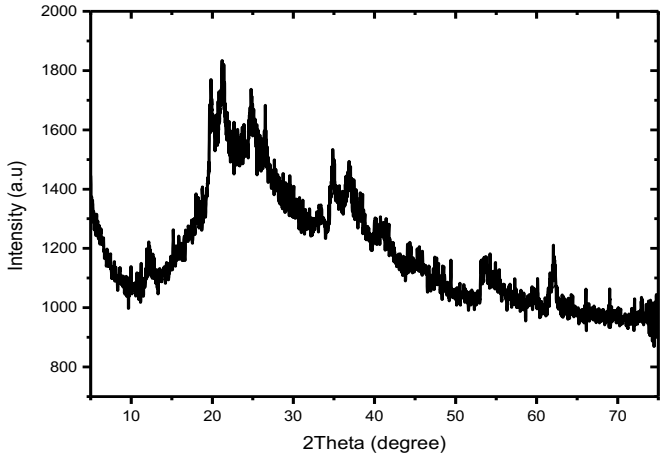

Figure 4: XRD pattern of EHA

3.2.3. Batch adsorption studies using EHA

The EHA was used for equilibrium adsorption studies to evaluate its adsorption potential for application to remove pollutants from waste water. The study investigated the effect of increasing adsorbent dosage, effect of increasing dye concentration and effect of solution pH on the adsorption of methylene blue from aqueous solution. Figure 7 shows the adsorption behaviour when amount of HA was gradually increased.

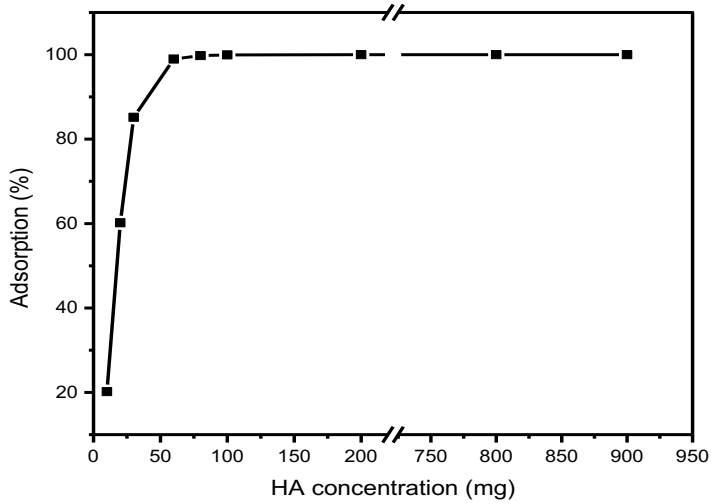

Figure 5: Effect of increasing adsorbent dosage on adsorption of MB onto EHA (Concentration of MB: 30 mg/L; adsorbent dosage 10 - 900mg; time 30 min at room temperature, 29 ±1˚C)

Significant increase in adsorption was observed as the HA concentration changed from 10 -100mg. Adsorption reached maximum in a system containing 100mg HA. At this dosage, all the dye molecules were removed from the system. Further increase in the adsorbent dosage had no effect on adsorption of MB indicated by a plateau after about 100% adsorption was achieved. The effect of initial concentration of MB was investigated with dye concentrations ranging from 2 to 30 mg/L using adsorbent dose of 50mg and stirred for 30 min at room temperature. The result (Figure 8) shows a decrease in adsorption as the concentration of MB was increased due to the gradual filling of the adsorption sites on the surface of the adsorbent [23]. Thus, the actual amount of MB adsorbed increases with time till the initial surface of the EHA becomes saturated.

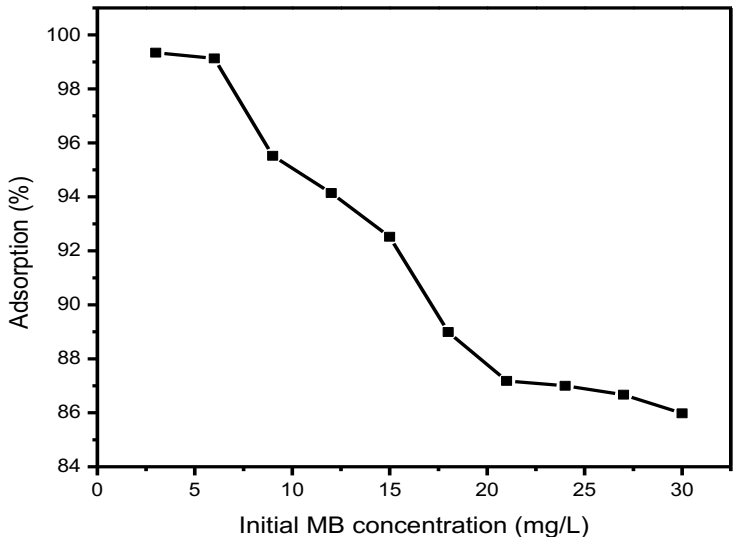

Figure 6: Effect of initial concentration of MB on adsorption onto EHA: (Concentration of MB: 3-30 mg/L; adsorbent dosage 50 mg; time 30 min at room temperature, 29 ±1˚C)

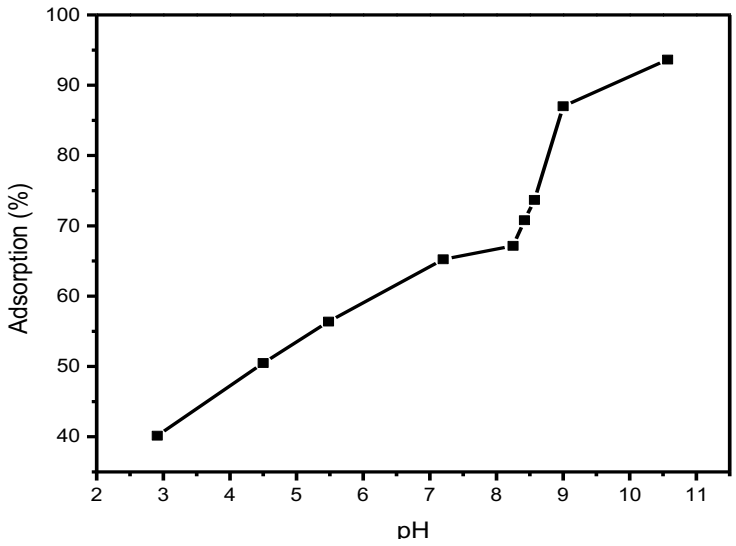

Figure 7: Effect of solution pH on adsorption of MB onto EHA (Concentration of MB: 30 mg/L; adsorbent dose 50mg; time 30 min at room temperature, 29 ±1˚C).

The effect of change in solution pH on the adsorption of MB onto HA is illustrated in Figure 9. The HA showed a gradual increase in adsorption as the pH increases with the maximum adsorption occurring in alkaline medium. This is because at low pH, the positive charge in the solution interface increases, thus, the adsorbent surface appears positively charged resulting in a decrease in adsorption potential [43]. While in alkaline medium, the positive charge on the adsorbent surface decreases, hence, the surface appears negatively charged [44, 45]. This enhances electrostatic attraction between the positively charged MB dye and the negatively charged adsorbent surface, thus, adsorption increases.

3.2.4. Equilibrium adsorption isotherms

The Langmuir, Freundlich and Temkin isotherms were used to study the adsorption mechanism of MB onto EHA. The parameters for each isotherm are presented in Table 5. The Langmiur model specifically applies to homogenous adsorption where all the adsorption sites possess equal affinity for the adsorbate with no transmigration in the plane of the surface. The mathematical expression for this model is given in Eq. 3, while the linear form is as represented in Eq. 4.

$$q_e = \frac{q_{max} K_L C_e}{1 + K_L C_e} \qquad (3)$$

$$\frac{C_e}{q_e} = \frac{1}{q_{max}\, K_L} + \frac{C_e}{q_{max}} \qquad (4)$$

Where q_{max} is the maximum monolayer adsorption capacity of the adsorbent, K_L is the Langmuir adsorption constant, which is related to the free energy of adsorption.

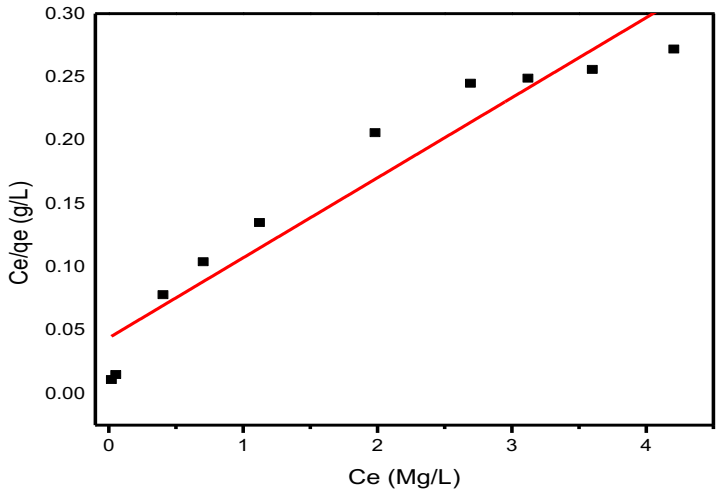

Figure 8: Langmuir's isotherm plot for the adsorption of MB onto HA

The Langmuir's isotherm plot (Figure 10) for the adsorption of MB onto EHA deviated from linearity, although exhibiting a correlation constant (R^2 = 0.925). This suggests that adsorption of MB onto the surface of the EHA was not monolayer, where adsorbed species could be possibly held to definite points of attachment on the surface of the adsorbent capable of accommodating one species per site. On account of the inapplicability of Langmuir isotherm to this process, an essential feature of the isotherm was determined in terms of a dimensionless parameter known as the separation factor (R_L= 0.023), which can be used to predict the nature of an adsorption. In this case, it describes the adsorption as favourable (0 < R_L < 1) rather than linear (R_L = 1) or unfavourable (R_L> 1) [46].Separation factor (RL) is given as:

$$R_L = \frac{1}{1 + K_L C_o} \qquad (5)$$

Where, Co is the adsorbate highest initial concentration and K_L is Langmuir adsorption constant.

The Freundlich empirical model applies to a multilayer adsorption with non-uniform distribution of adsorption heat and affinities over a heterogeneous surface. The plot of this isotherm is given in Figure 11. The linearized form of the model is given as:

$$Inq_e = InK_f + \frac{1}{n} InC_e \qquad (6)$$

The slope (1/n) of the Freundlich isotherm plot is an indication of surface heterogeneity, which increases as 1/n tends to zero. As shown in Table 5, 1/n = 0.362 and R^2 value of 0.971 suggests more of the Freundlich isotherm behaviour than the Langmuir and Temkin isotherms. Thus, the adsorption process could be best described as a multilayer adsorption.

The Temkin's isotherm model explains the effect of an indirect adsorbent-adsorbate interactions in the adsorption system. It also suggests that the heat of adsorption of all the molecules would decrease linearly with coverage due to these interactions. The expression of this model is given as:

$$q_e = B_1 InK_1 + B_1 InC_e \qquad (7)$$

Where B_1 is Temkin's constant related to the heat of adsorption and $K_1$is the equilibrium binding constant. The plot of this isotherm is shown in Figure 12. The isotherm parameters (Table 5) indicate that the heat of adsorption of all molecules in the system decreases linearly with coverage as a result of adsorbent-adsorbate interaction which is characterized by a uniform distribution of its bonding energies down to 2.274 J/mol

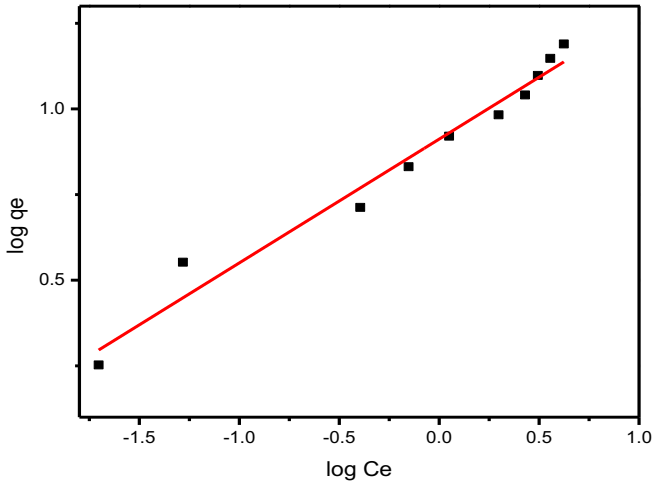

Figure 9: Freundlich's isotherm plot for the adsorption of MB onto HA

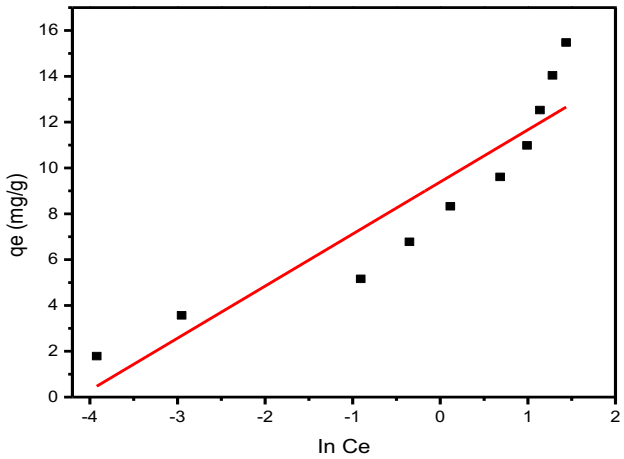

Figure 10: Temkin's isotherm plot for the adsorption of MB onto HA

Table 4: Isotherm parameters for adsorption of MB onto HA

Isotherm	Parameter	Value
Langmuir	q_{max} (mg/g)	15.820
	K_L(L/mg)	1.439
	R_L	0.023
	R^2	0.925
Freundlich	K_F ($mg^{1-1/n} L^{1/n} g^{-1}$)	8.279
	n	2.766
	R^2	0.971
	1/n	0.362
Temkin	K_T (L/g)	62.214
	B_1 (J/mol)	2.274
	R^2	0.861

Table 6: Comparison of Langmuir adsorption capacities of different adsorbents for the removal of MB

Adsorbent	q_{max} (mg/g)	References
Activated carbon	17.63	[47]
Class fly ash	4.92	[48; 49]
Raw beach saw dust	9.78	[50]
Cotton stalk	11.60	[51]
Coconut coir	15.59	[52]
Fly ash-HNO_3	7.74	[53]
Humic acid	15.82	This study

Conclusion

The use of HA extracted from benthic sediment from the river as an eco-friendly and low cost adsorbent for the removal of methylene blue from aqueous solution achieved a remarkable adsorption potential. The extraction process gave a low yield of HA (4.89%) due to a strong affinity of the HA to the fulvic acid fraction. Characterization reveals the extracted HA, as the commercial one, is a complex organic compound, consisting of pores with a host of organic functionalities. A very low concentration of HA (100 mg) afforded adsorption close to 100% within 30 min. Adsorption of methylene blue onto HA is highly favoured in alkaline medium as a result of increase in the electrostatic attraction between the positively charged dye and the negatively charged HA surface. Freundlich isotherm model provided the best fit (R^2 = 0.971), suggesting a multilayer adsorption. This study indicates that HA extracted from sediments is a potential low cost adsorbent for the removal of cationic dyes from aqueous solution.

Acknowledgements-The authors acknowledge the support by the Ministry of Science and Technology in South Korea through the Institute of Science and Technology for sustainability (UNU & GIST joint programme).

References

1. Y. Shevah, Water Resources, Water Scarcity Challenges, and Perspectives, In: Water Challenges and Solutions on a Global Scale, American Chemical Society, 2015, pp. 185.
2. S.O. Wandiga, *In Water Challenges and Solutions on a Global Scale* (2015).
3. A. Roy, B. Adhikari, S. Majumder, *Ind. Eng. Chem. Res.* 52 (2013) 6502.
4. Q. Hu, S. Qiao, F. Haghseresht, M. Wilson, G. Lu, *Ind. Eng. Chem. Res.* 45 (2006) 733.
5. M.H. Karaoğlu, M. Doğan, M. Alkan, *Ind. Eng. Chem. Res.* 49 (2010) 1534.
6. F. Tümsek, O.Z. Avcı, *J. Chem. Eng. Data* 58 (2013) 551.
7. Y. El Mouzdahir, A. Elmchaouri, R. Mahboub, A. Gil, S. Korili, *J. Chem. Eng. Data* 52 (2007) 1621.
8. L.S. Oliveira, A.S. Franca, T.M. Alves, S.D. Rocha, *J. Hazard. Mater.* 155 (2008) 507.
9. J. Ma, F. Yu, L. Zhou, L. Jin, M. Yang, J. Luan, Y. Tang, H. Fan, Z. Yuan, Chen J., *ACS appl. mater. interfaces* 4 (2012) 5749.
10. F. Fu, Z. Gao, L. Gao, D. Li, *Ind. Eng. Chem. Res.* 50 (2011) 9712.
11. H. Shi, W. Li, L. Zhong, C. Xu, *Ind. Eng. Chem. Res.* 53 (2014) 1108.
12. M.T. Yagub, T.K. Sen, S. Afroze, H.M. Ang, *Adv. Colloid Interface Sci.* 209 (2014) 172.
13. S. Wang, Z. Zhu, A. Coomes, F. Haghseresht, G. Lu, *J. Colloid Interface Sci.* 284 (2005) 440.
14. F.A. Pavan, E.C. Lima, S.L. Dias, A.C. Mazzocato, *J. Hazard. Mater.* 150 (2008) 703.
15. O. Hamdaoui, *J. Hazard. Mater.* 135 (2006) 264.
16. E. Rubin, P. Rodriguez, R. Herrero, J. Cremades, I. Barbara, S. de Vicente, E.Manuel, *J. Chem. Technol. Biotechnol.* 80 (2005) 291.
17. S. B. Bukallah, M. Rauf, S. AlAli, *Dyes and Pigments* 74 (2007) 85.
18. R. Han, Y. Wang, X. Zhao, Y. Wang, F. Xie, J. Cheng, M. Tang, *Desalination* 245 (2009) 284.
19. D. Özer, G. Dursun, A. Özer, *J. Hazard. Mater.* 144 (2007) 171.
20. U. Etim, S. Umoren, U. Eduok, *J. Saudi Chem. Soc.*20 (2016) S67.
21. E. Inam, U. Etim, E. Akpabio, S. Umoren, *J. Taibah Univ. Sci.* (2016).
22. S. Umoren, U. Etim, A. Israel, *J. Mater. Environ. Sci.* 4 (2013) 75.
23. E.J. Inam, U.J. Etim, E.G. Akpabio, S.A. Umoren, *Desalination and Water Treatment* 57 (2016) 6540.
24. I. Ali, *Chem. Rev.* 112 (2012) 5073.
25. S.S. Shenvi, A.M. Isloor, A.F. Ismail, S.J. Shilton, A. Al Ahmed, *Ind. Eng. Chem. Res.* 54 (2015) 4965.
26. Z. Sun, B. Tang, H. Xie, *Energy Fuel* 29 (2015) 1269.

27. P. Wu, Q. Zhang, Y. Dai, N. Zhu, Z. Dang, P. Li, J. Wu, X. Wang, *Geoderma* 164 (2011) 215.
28. X. Zhang, P.Zhang, Z. Wu, L. Zhang, G. Zeng, C. Zhou, *Colloids Surf. Physicochem. Eng. Aspects* 435 (2013) 85.
29. Y. Zhang, Q. Li, L. Sun, R. Tang, J. Zhai, *J. Hazard. Mater.* 175 (2010) 404.
30. W.W. Tang, G.M Zeng, J.L. Gong, J. Liang, P. Xu, C. Zhang, B.B. Huang, *Sci. Total Environ.* 468 (2014) 1014.
31. F.J. Stevenson, Humus chemistry: genesis, composition, reactions, John Wiley & Sons, 1994.
32. W. Robinson, *J. agric. Res* 34 (1927) 339.
33. N. Barot, H. Bagla, *Green Chem. Lett Rev.* 2 (2009) 217.
34. P. Warwick, E. Inam, N. Evans, *Environ. Chem.* 2 (2005) 119.
35. O. Purmalis, M. Klavins, *ESJ* (2013).
36. M. Thommes, K. Kaneko, A.V. Neimark, J.P. Olivier, F. Rodriguez-Reinoso, J. Rouquerol, K.S. Sing,*Pure Appl. Chem.* 87 (2015) 1051.
37. Q. Wei, D. Yang, T.E. Larson, T.L. Kinnibrugh, R. Zou, N.J. Henson, T. Timofeeva, H. Xu, Y. Zhao, B.R. Mattes, *J. Mater. Chem.* 22 (2012) 10166.
38. T. Gierlach-Hladon, L. Szajdak, (2010). Available online http://agris.fao.org/agris-search/search.do?recordID=LV2010000341
39. S.S. Fong, L. Seng, W.N. Chong, Asing J., *J. Braz. Chem. Soc.* 17 (2006) 582.
40. N. Tomar, R. Yadav, P. Relan, *Arid Land Res. Manage.* 6 (1992) 187.
41. A. Naidja, P. Huang, D. Anderson, C. Van Kessel, *Appl. Spectrosc.* 56 (2002) 318.
42. T. Zuyi, L. Shifang, Z. Jianjun, S. Fenling, *Chem. Ecol.* 13 (1997) 237.
43. A. Mittal, *Electron. J. Environ. Agric. Food Chem.* 5 (2006) 1296.
44. J.F. Osma, V. Saravia, J.L. Toca-Herrera, S.R. Couto, *J. Hazard. Mater.* 147 (2007) 900.
45. M.A.M. Salleh, D.K. Mahmoud, W.A. Karim, A. Idris, *Desalination* 280 (2011) 1.
46. K. Foo, B. Hameed, *Chem. Eng. J.* 156 (2010) 2.
47. B.J. Acemioglu, *J.Colloid Interface Sci.* 274 (2004) 371-379.
48 S. Wang, Y. Boyjoo, A. Chouei, Z.H. Zhu, *Water Res.* 39 (2005): 129-138.
49 N.A. Oladoja, I.O. Raji, S.E. Olaseni, T.D. Onimisi, *Chem. Eng. J.* 171 (2011) 941-950
50 F.A. Batzias, D.K. Sidiras, *J. Hazard. Mater.* 114 (2004) 167-174
51 M. Ertas, B. Acemioglu, M.H. Alma, M. Usta, *J. Hazard. Mater.* 185 (2010) 421-427.
52 Y.C. Sharma, S.N. Uma, Upadhyay., *Energy Fuels* 23 (2009) 2983-2988
53 S. Karaca, A. G€urses, M. Acikyildiz, M. Ejder, *Microp. Mesop. Mater.* 115(2008) 376-438.

(2018) ; http://www.jmaterenvironsci.com